

OBSTACLE GAIN AT MICROWAVE FREQUENCIES

Samuel R. Bradshaw
Motorola Inc.
Riverside Research Laboratory
Riverside, California

Summary

Calculations of expected transmission loss over a single obstacle path show that if conditions are right the loss will be less than if the obstacle were not there. Compared to diffraction loss over a smooth earth, this so-called "obstacle gain" can be appreciable. During 1957, a study and experimental investigation of the obstacle gain effect in the microwave region was completed. This paper discusses experimental methods and results, describes siting and prediction techniques, and outlines the instrumentation employed in the program. Theoretical and measured losses were in good agreement.

Introduction

Theoretical predictions and confirming measurements have demonstrated that obstructed paths for terminals below the radio horizon may exhibit lower transmission loss figures than propagation over the equivalent smooth earth path. This decrease in transmission loss has been termed "obstacle gain."

Just as light waves are diffracted by a straight edge, radio waves are bent slightly when a mountain ridge lies across the propagation path. Depending upon the sharpness of the top of the ridge and diffraction angle involved, one of several methods can be used to predict the path loss for such a radio circuit. Three such methods will be discussed in a later section of this paper.

In 1955, under Contract No. DA-36-039 SC-64556, Motorola Riverside Research Laboratory conducted an experimental investigation of mountain obstacle path transmission.^{1,2} The frequencies used in the measurements program were largely in the 50 to 500 Mc region with a limited number of checks at 932 Mc and 1865 Mc. Results were quite favorable with the result that the Signal Corps issued a new contract (DA-36-039 SC-73057)³ for continuing the study in the frequency range 1700 to 8500 Mc. Many of the same obstacle paths that proved successful at the lower frequencies have also been usable at microwave frequencies.

Before presenting some of the test results of the present measurements program, a description of the physical equipment and its parameters will be given. A block diagram of the transmitting equipment is shown in Figure 1.

At 2450 Mc, the lowest of the microwave test frequencies, a 4J61 is the transmitting magnetron with an output of nearly 50 watts cw. The output is fed to a coupler which transforms from 7/8-inch to 3/8-inch coaxial line and then through a directional coupler to the dipole-disc feed for the 4-foot parabolic reflector. The -30 db branch of the coupler is connected to a crystal detector and the rectified crystal current is used as a monitor of the magnetron output power. The power supply, modulator, antenna elevation angle control switches, and power output meter are placed at the operating position inside the transmitter van. The magnetron, directional coupler, and crystal detector are mounted on the back of the parabolic reflector.

To convert the transmitter for operation at 4000 Mc, only the magnetron and dipole-disc feed are changed. A QK-117A magnetron with an output of approximately 30 watts cw is used at this frequency.

At 8250 Mc, the output of a QK-261 or -262 magnetron is fed into a 2-hole directional coupler with 30 db attenuation to the power monitoring crystal detector. A Cutler feed is used with the 4-foot parabolic reflector as the antenna system.

The antenna is mounted on a rotary milling table, and hence accurate azimuth settings can be maintained and repeated. For the first few measurements in the program a TV type rotator was used, but gear slop and difficulty of returning to exact azimuth settings necessitated the use of a more precise method of azimuth alignment.

Figures 2 and 3 are block diagrams of the receiving and calibration equipment. The 2450 Mc and 4000 Mc systems are identical except for the local oscillator frequency and dipole-disc antennas. The directional couplers are so arranged that the received signal feeds through to the crystal detector with negligible attenuation. The output of the klystron oscillator appears at the mixer crystal after being attenuated 20 db by the directional coupler. In the direction of the antenna this same signal is attenuated a minimum of 40 db. For signal strength calibration purposes, the output of the signal generator appears at the detector after suffering 20 db attenuation in the directional coupler. An additional 20 db

loss (minimum) in coupling to the antenna due to the properties of the directional coupler prevents radiation of the calibrating signal from affecting the accuracy of measurement.

The output signal from the crystal detector is fed to the IF amplifier. The IF amplifier has a bandwidth of approximately 2.5 Mc, a noise figure of better than 2 db, and a gain of 95 db. The AGC voltage is plotted using the Sanborn pen recorder and gives a direct indication of the received signal strength. An audio output from the IF amplifier and detector is also brought to the operating position to aid in locating and identifying weak signals.

The receiving system for 8250 Mc utilizes the same parabolic reflector as at the other test frequencies but uses waveguide plumbing rather than coaxial components. The parabolic reflector focuses the received signal at the input of the Cutler feed and the path is thence through a 2-hole directional coupler in the direction of negligible attenuation to a harmonic mixer. The output of the klystron oscillator is set to 4125 Mc \pm 15 Mc and fed to the harmonic mixer, the output of which goes to the 30-Mc IF amplifier. For calibration purposes, the output of the signal generator is introduced through the -18 db leg of the directional coupler. The remainder of the system is as previously described for the two lower frequencies. By using the harmonic mixer, only one local oscillator is required for all three frequencies and this, of course, simplifies the equipment requirements and operational procedure.

Equipment characteristics were such that path losses of at least 200 db could be measured at any of the test frequencies.

A photographic view of the interior of the transmitter truck is shown in Figure 5. The magnetron power supply is mounted just above the operator's table and the modulation control is located just above the meters and centered on the panel.

The interior views of the receiving van (Fig. 6) illustrate how the signal generators, recorder, and klystron local oscillator are mounted. In addition, the dipole-disc and Cutler feeds as well as the directional coupler and crystal mixer assemblies are shown.

Primary power for operating the equipment is furnished by a 1500-watt portable gasoline generator. A tower, variable in height from 14 to 23 feet, is mounted at the rear of each van (Fig. 4).

As indicated in the block diagrams, 47.7 Mc transceivers are employed for 2-way voice communication in the coordination of the microwave measurements. Quad antennas are used with this equipment to achieve the extra gain necessary on the higher loss paths.

Prediction Methods

If the ridge approaches a knife edge at the frequency involved and the diffraction angle is quite small (a maximum of 5° or 6°), the Fresnel integral can be used to determine the amplitude coefficient and the total phase shift along the path. In order for the knife edge diffraction formula to be valid, the distances from the transmitter and receiver to the obstacle must be large compared to obstacle height, and this height must be large compared to a wavelength. The horizontal extension of the knife edge theoretically should be infinite, but practically it need only be large compared with obstacle height. If the above two conditions are met, the field at the receiver is given by

$$E = E_0 \frac{e^{j\pi/4}}{\sqrt{2}} \int_{-\infty}^{\nu} e^{-j\pi v^{2/2}} dv$$

where E_0 is the field that would exist at the receiver under free space conditions and

$$\nu = \pm H_D \sqrt{\frac{2}{\lambda} \left(\frac{1}{d_1} + \frac{1}{d_2} \right)}$$

In the above formula d_1 and d_2 are the distances from transmitter and receiver to the obstacle, and H_D is the effective obstacle height. If the receiver is in the shadow zone behind the ridge, so that $\nu < -2$, then the following approximate formula holds

$$C = \left| \frac{E}{E_0} \right| = \frac{0.225}{\nu}$$

Substituting the value of ν as previously defined and expressing logarithmically $20 \log C = 10 \log D + 20 \log H_D + 10 \log F_{mc} - 10 \log d_1 - 10 \log d_2 - 51.2$. Total path loss would thus be the loss due to diffraction over the knife edge obstacle as determined above plus the free space path loss. (Transmission loss in free space can be expressed as

$$\frac{P_t}{P_r} = \frac{(4 \pi D)^2}{\lambda^2}$$

where P_t is radiated power and P_r is power available at the receiving antenna. Expressed in db, $L_b = 20 \log d + 20 \log F_{mc} + 36.6$. A nomogram for determining knife edge diffraction loss and free space path loss is shown in Figure 7.

If reflection points are present on both sides of the obstacle and antenna heights are

optimized a possible 12 db improvement in total path loss figure is predicted by h-ray theory. However, we were unable to find a path which exhibited such an improvement during the measurements program.

When a double obstacle path is to be used, an extension of the 20 log C prediction method gives a good estimate of the path loss. Loss over the first obstacle is determined using the transmitter and the peak of the second obstacle as terminal points. Similarly, using the top of the first obstacle and the receiver location as terminals, diffraction loss over the second peak is found. The free space path loss over the entire distance between transmitter and receiver is then added to the two diffraction losses to give the total predicted loss.

Experimental results indicate that radio waves are attenuated due to absorption and possibly other causes if the wave propagates close to the surface of the earth for any appreciable distance. This attenuation increases with frequency. If the obstacle were spherical rather than a knife edge at the frequency being used or if the diffraction angle were too great, the ray would probably graze the surface for some distance. For such a case, knife edge diffraction theory would not predict sufficient path loss and a different prediction method would be advisable. A prediction method which assumes diffraction by a spherical obstacle, adapted from the general solution by Messrs. van der Pol and H. Bremmer, has been proposed and seems to offer considerable merit.

Path loss due to diffraction assuming a spherical obstacle would be

$$L_S = 3.4 n^{1/2} \frac{e^{-1.84 f_2(\delta) n}}{\sqrt{[f_1(\delta) - \Delta]^2 + f_2(\delta)^2}} \quad (1)$$

$\Delta \gg f_1(\delta)$ or $f_2(\delta)$, hence

$$\sqrt{[f_1(\delta) - \Delta]^2 + f_2(\delta)^2} \cong \Delta$$

and

$$L_S = 3.4 n^{1/2} \frac{e^{-1.84 f_2(\delta) n}}{\Delta} \quad (2)$$

where $f_2(\delta) = 1.56$, $\Delta = .356 H^{-2/3} \lambda^{-2/3} T^{4/3}$

and $n = \frac{d}{2d_1 d_2} (2 H_D T)^{2/3} \lambda^{-1/3}$.

H_D , the obstacle height, λ the wavelength, T the obstacle thickness, and d the path length must be in the same units.

If $d_1 = d_2$ (obstacle at midpath) and $T = .185 H$, then

$$n = \frac{1.03 H_D^{4/3}}{d \lambda^{1/3}}$$

and

$$\Delta = .61 \frac{H_D^{2/3}}{\lambda^{2/3}}$$

Substituting these values in formula (2) and changing to frequency in megacycles and distance in miles, we get

$$L_S = \frac{2.42 e^{-2.87}}{F^{1/2} d^{1/2}}$$

or changing signs and expressing conventionally as a loss in decibels

$$L_S = 25 + 10 \log F + 10 \log d - 7.7 \quad (3)$$

The total loss L_S can be divided into two parts, $L_{S1} = 25$ and $L_{S2} = 10 \log F + 10 \log d - 7.7$. Nomograms for determining L_{S1} and L_{S2} appear as Figures 8 and 9. For total path loss, of course, the spherical diffraction loss is added to the free space loss of the path being investigated.

The preceding two prediction methods both have theoretical justification and for this reason should be used where practicable. However, an average path loss value based on a number of actual field measurements should be of value in preliminary estimates of the usefulness of a path. Based on a series of measurements over 39 different obstacle paths, 50 db should be added to the free space loss in the 2000-5000 Mc frequency range and 56 db in the 5000-8500 Mc band.

Siting Techniques

Once it has been determined that a suitable obstacle path exists and predictions have been made to see if the available equipment can operate satisfactorily over such a path, the following siting techniques proved useful during the measurements program:

1. Since it is difficult to survey over an appreciable area using microwave equipment and associated highly directional antennas, the actual signal strength surveys are conducted using VHF equipment and nondirectional or wide beamwidth antennas.

2. The transmitter truck tentatively selects a location and transmits VHF carrier while the receiver truck surveys the other terminal area to find maximum signal strength spots.

3. When a "hot spot" is found at a location suitable for setting up, the receiver truck may transmit test signals at VHF if a more suitable location is required at the transmitter end.

4. When both locations are determined, the microwave equipment is put into operation after taking special care in antenna alignment. The following procedure was used in antenna alignment:

a. The bearing between the terminals is determined from the map.

b. With the aid of a Brunton compass or transit, the point on the obstacle to which the antenna should be aimed is determined.

c. A sighting is made across the periphery of the dish to the obstacle and the antenna is then turned 90° to properly line up in azimuth with the desired path. Alternatively, a sighting can be made on a point 90° from the desired path and the antenna would not have to be rotated. Elevation alignment is achieved by boresighting to the top of the obstacle through the antenna opening of the parabolic reflector.

d. Since there is usually slight error in the map bearing final azimuth alignment is accomplished by maximizing on a signal.

5. It may be necessary to change antenna heights to receive an optimum signal. Moving the truck a short distance would accomplish the same purpose where it is not convenient to vary height.

Test Results

Figure 10 is a simplified map of the test area. Paths tested varied in length from about 6 miles to over 150 miles. The path terrain varied from barren desert type to wooded and snow-covered types. One path was tested after a moderately heavy snow and later when the snow was melted from the ridge. There was very little difference in measured path losses on the two occasions.

Profiles of four paths are shown in Figures 11 through 14. The first two are paths more than 100 miles long which were successfully tested at 2450 Mc. The third profile is for a path nearly 50 miles in length, the longest path that was successfully negotiated at all three test frequencies. The last profile is for a double obstacle path and was successfully tested only at 2450 Mc. Path loss was 24 db more than predicted by the knife edge theory for the path assuming only a single obstacle was present.

Several 24-hour checks have been made, two or more at each microwave test frequency. On a 17-mile path with no reflection points on either side of the obstacle, variation at all three test frequencies was no more than ± 3 db. On longer paths, with and without reflection points, variation was as much as ± 10 db over a 24-hour test period.

It has become evident as a result of a good number of path loss measurements that it is important to maintain low diffraction angles on obstacle paths. Even on comparatively short paths if the total diffraction angle is greater than 5 to 6 degrees, path loss is much greater than predicted by knife edge diffraction theory. For long paths, beyond about 30 miles, it is best to keep this total angle under 4 degrees.

Predictions of expected path loss over a single obstacle or short double-obstacle path can be made with considerable accuracy. Predicted values were within 0.7 db of measured path losses using the spherical diffraction method, with a small and consistent spread on both sides of actual path losses. Knife edge predictions were, on the average, about 9.0 db low. However, a constant correction factor would be in order here, since the predicted path loss was below the measured loss for nearly every path tested. Eight double-obstacle paths were checked and predictions averaged within 3.5 db of measured path loss.

Conclusions

Among the more important findings of the measurement and study program are the following:

- (1) Fully reliable medium to long range point-to-point microwave communications in mountainous areas can be established over obstructed transmission paths.
- (2) Although not all obstructed paths are useful, the feasibility of attempting communications over a given path can be determined from the $4/3$ earth radius profile. Best terminal sites can be consistently predicted to within one mile.
- (3) Mountain obstacle transmission paths display broadband frequency characteristics covering the frequency range 50 - 8500 Mc as long as the total diffraction angle is less than 6° . For greater angles, successful paths could probably be established in the VHF and low UHF regions.
- (4) Successful techniques have been developed during the experimental program for siting obstacle path terminals and predicting requirements and performance. The straightforward procedures may be readily adapted to field use.
- (5) Fade range over a 24-hour period on paths where there is negligible multipath effect is not over ± 3 db. If multipath transmission takes place, the fade range may be as much as ± 10 over a 24-hour period.
- (6) The type of surface cover (rocky, snow, barren, or wooded) at the crest of the obstacle does not seem to be of importance.
- (7) Short double-obstacle paths have approximately 1.25 times the db diffraction loss exhibited by single obstacle paths.

(8) Where suitable terrain exists, obstacle circuits represent a considerable saving in installation and equipment costs compared with tropospheric scatter installations.

Acknowledgments

The author would like to express his gratitude to his coworkers at Motorola Riverside Research Laboratory who have participated in this investigation. Thanks are also due to Chester E. Sharp, Project Engineer for the U.S. Army Signal Research and Development Laboratory, and his associates, for their support and suggestions during the course of the program.

References

1. R. E. Lacy, "Mountain Obstacle Measurements," paper presented at the March 1957 IRE National Convention and published in the Convention Record, Vol. 5, Part 1.
2. H. R. Austin, R. E. Baker, S. R. Bradshaw,

J. M. Hollinrake, W. L. Jewell, and D. E. Moore, "Experimental Investigation of Mountain Obstacle Path Transmission." Motorola, Inc., Riverside Research Laboratory, Final Report, Signal Corps Contract No. DA-36-039 SC-64556, November 1955.

3. S. R. Bradshaw, P. L. Cassell, J. H. Craig, W. R. Kerley, and D. E. Moore, "Experimental Investigation of Mountain Obstacle Path Transmission at Microwave Frequencies," Motorola Inc., Riverside Research Laboratory, Final Report RL-3824-4, Signal Corps Contract No. DA-36-039 SC-73057, August 1957.
4. C. R. Burrows and S. S. Attwood, "Radio Wave Propagation," Academic Press, 1949, pp 462-464.
5. S. Matsuo, "The Method of Calculating VHF Field Intensity and Research on its Variation," The Electrical Communications Laboratory, Ministry of Telecommunications, Japan, 1950.

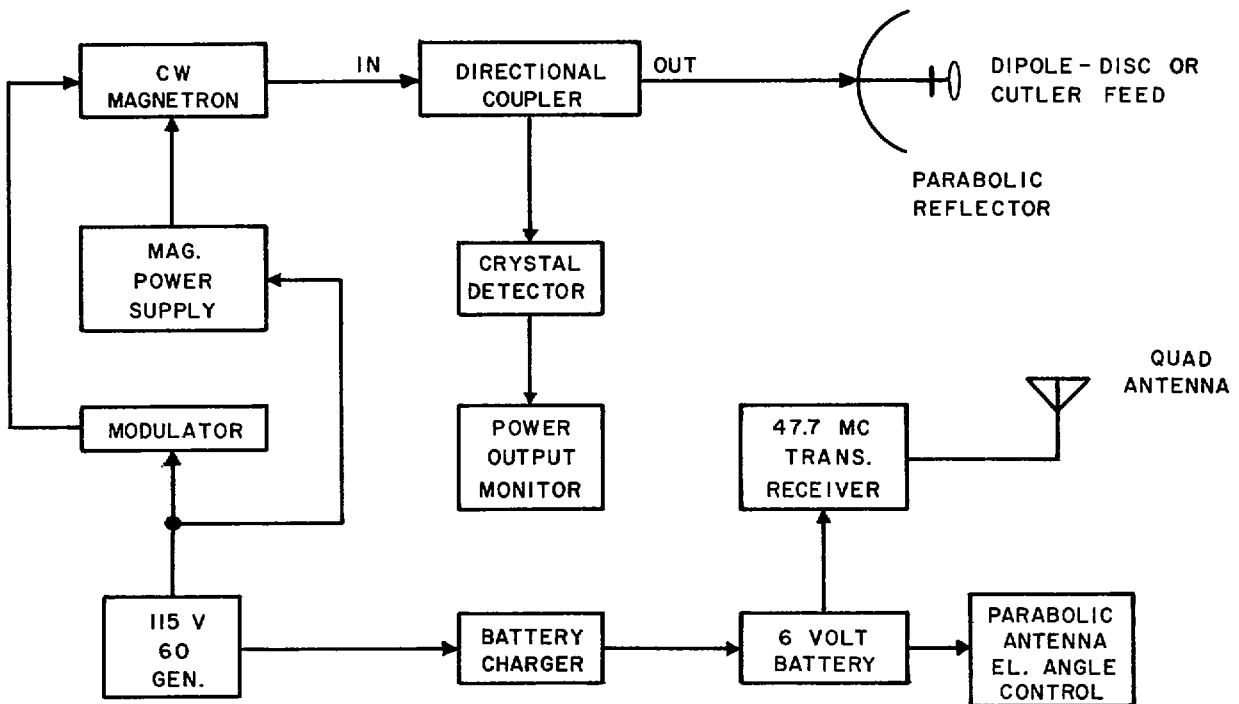


Fig. 1. Block diagram of microwave transmitting terminal equipment.

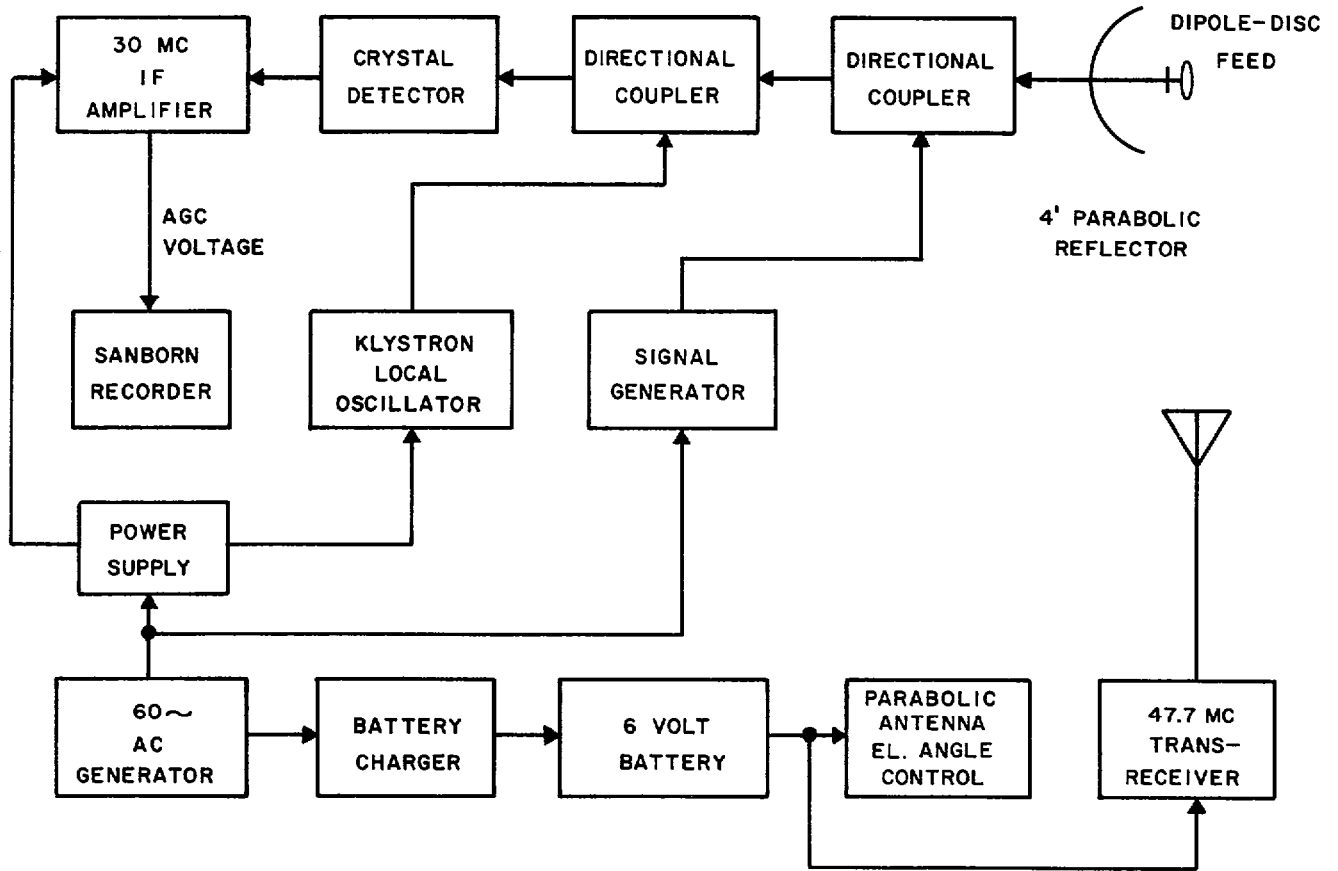


Fig. 2. Block diagram of 2,450 mc and 4,000 mc receiving terminal equipment.

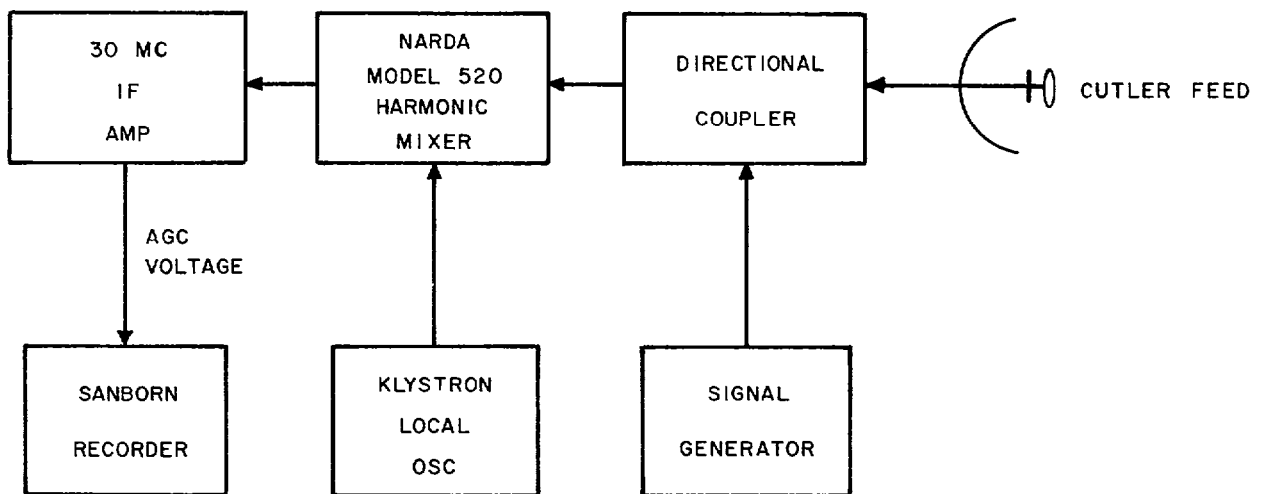


Fig. 3. Simplified block diagram of 8,250 mc receiving terminal equipment.

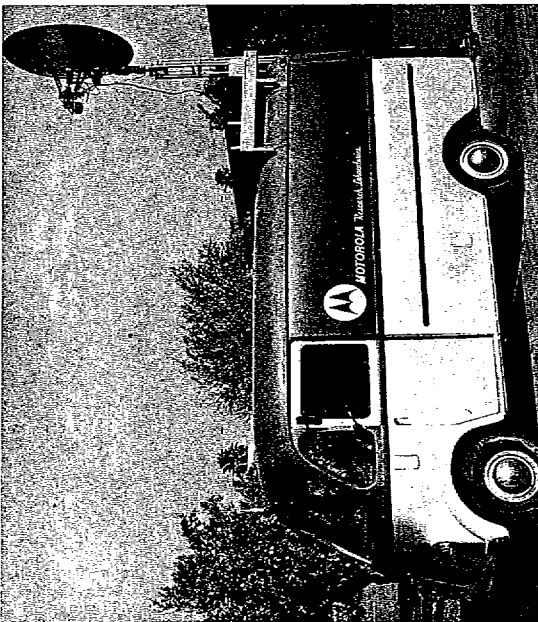


Fig. 4. Transmitter truck with parabolic antenna in place.

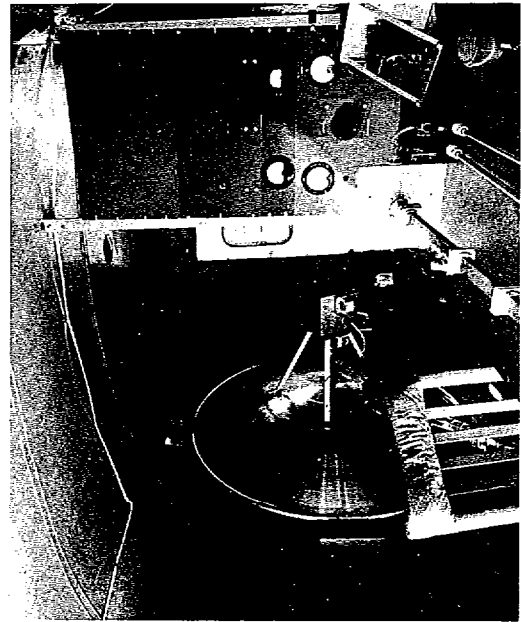


Fig. 5. Interior view of transmitter truck.

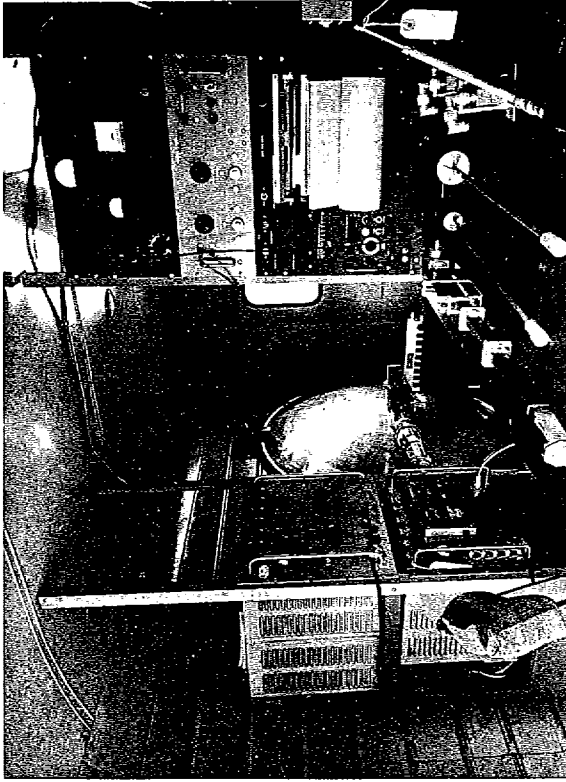


Fig. 6a. Interior view, receiver truck.

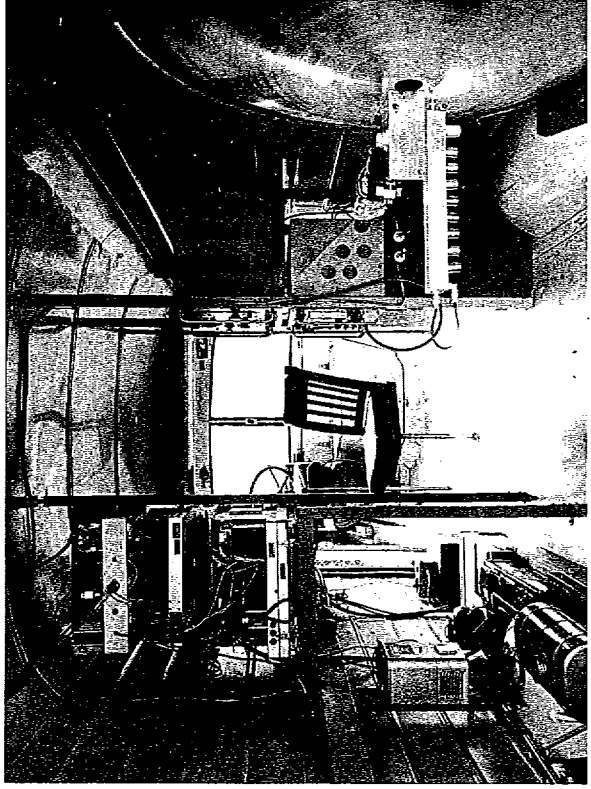


Fig. 6b. Interior view, receiver truck.

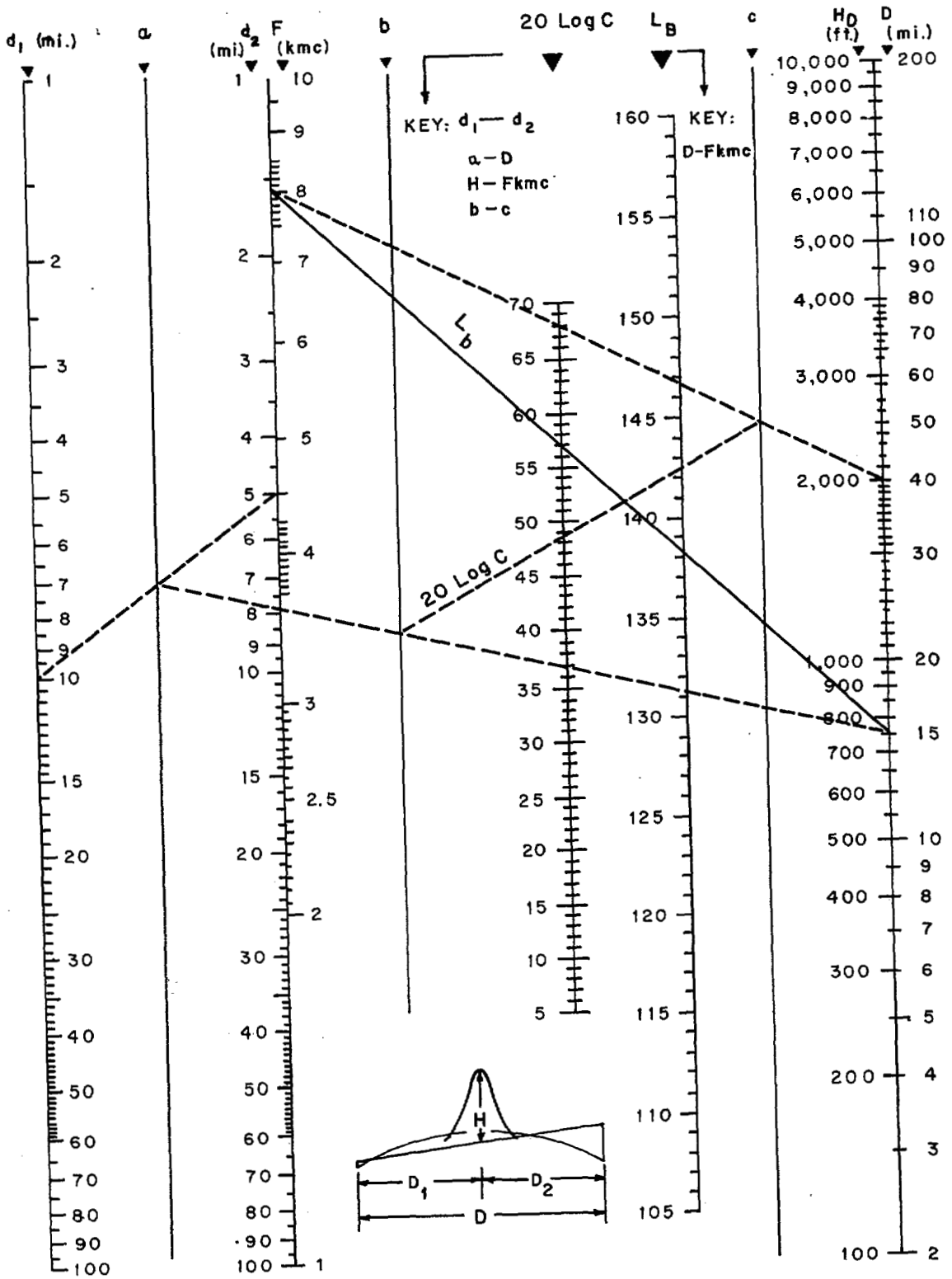


Fig. 7. Nomograms for use in estimating diffraction and free-space loss.

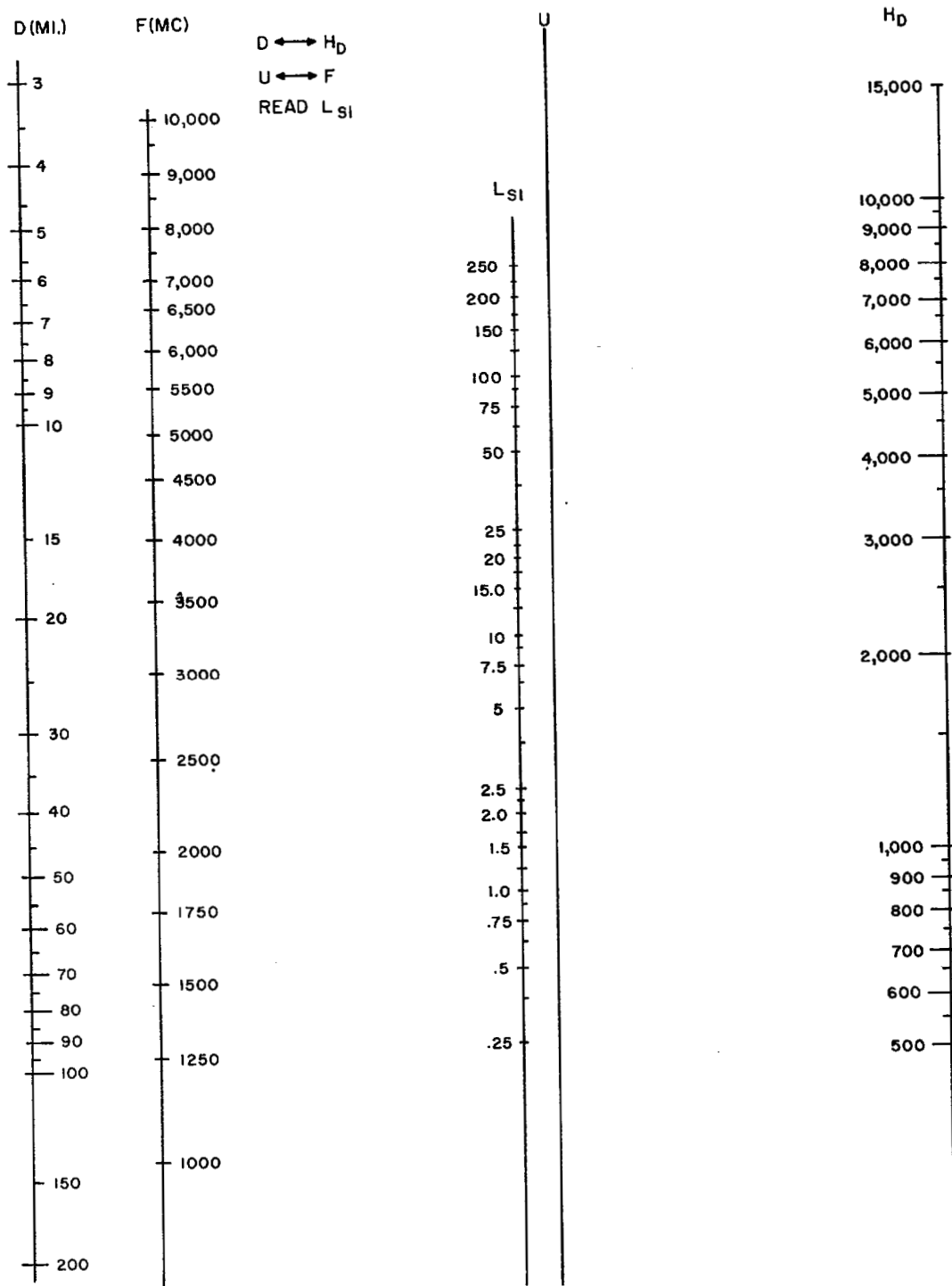


Fig. 8. Nomogram for L_{SI} .

D ↔ F
READ L_{S2}

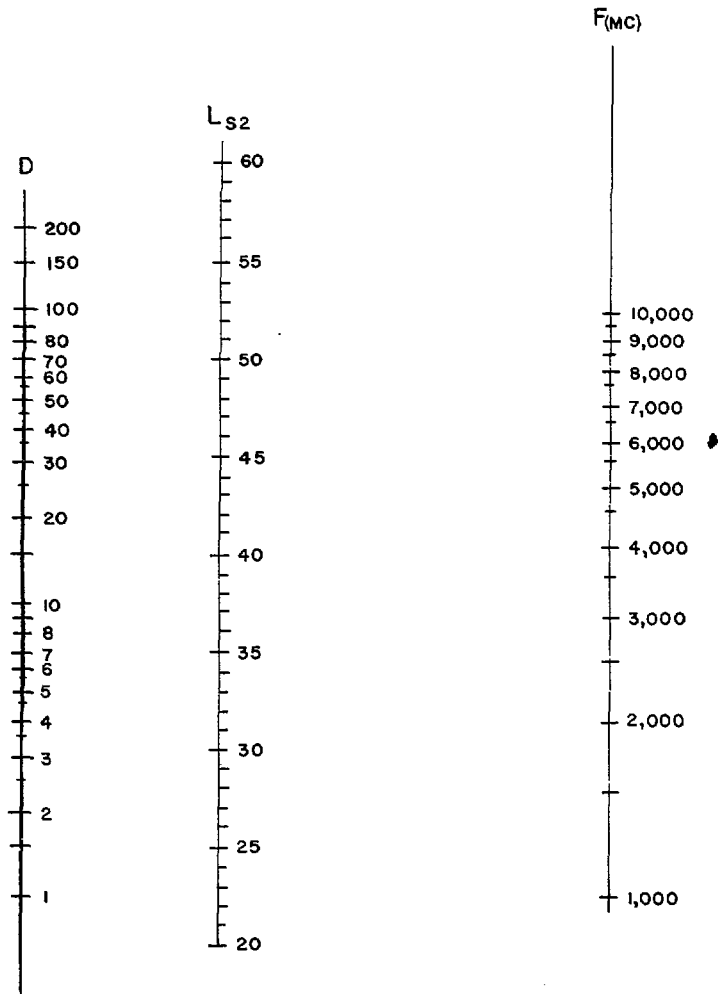


Fig. 9. Nomogram for determination of L_{S2} .

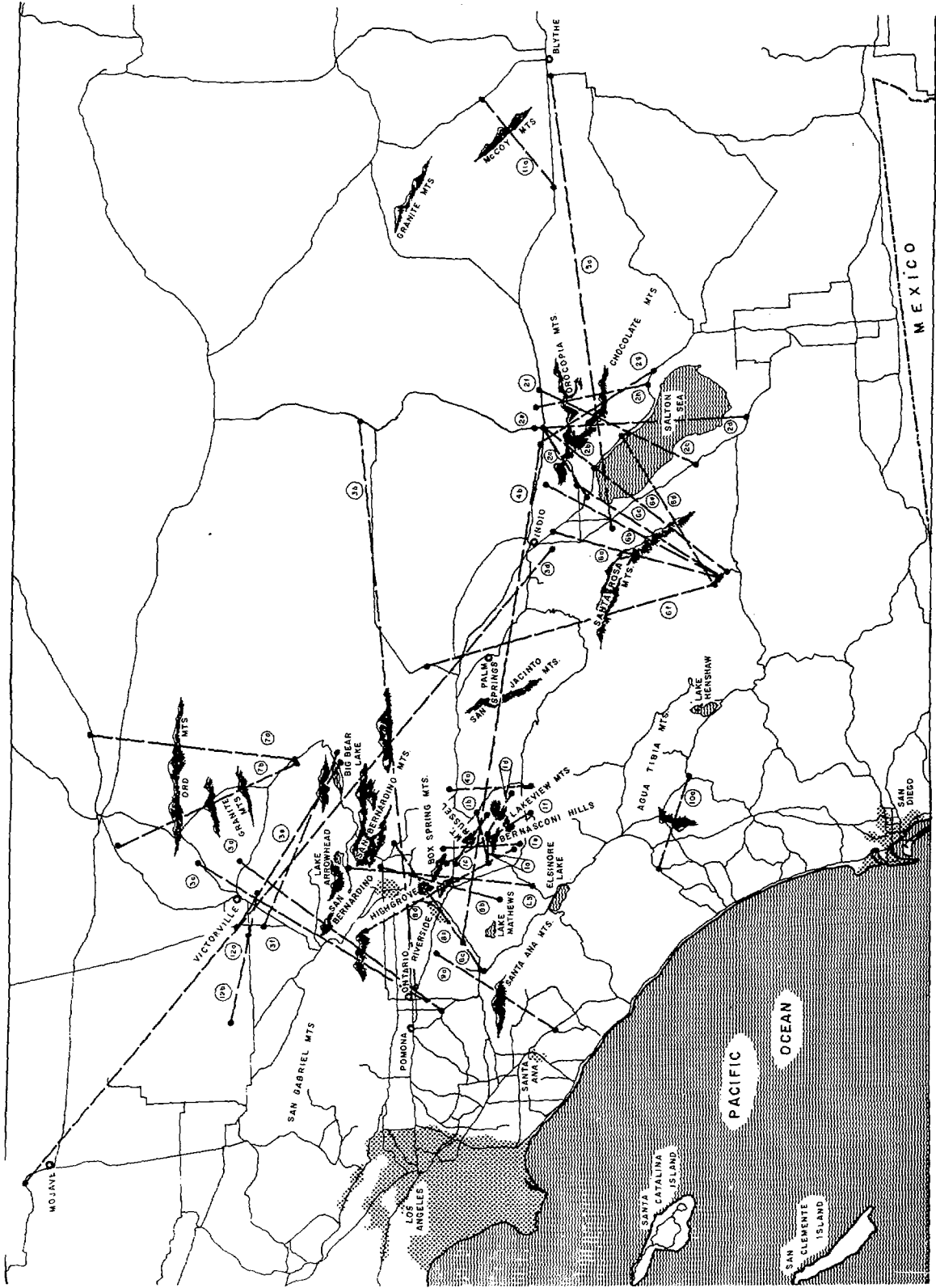


Fig. 10. Map of test area.

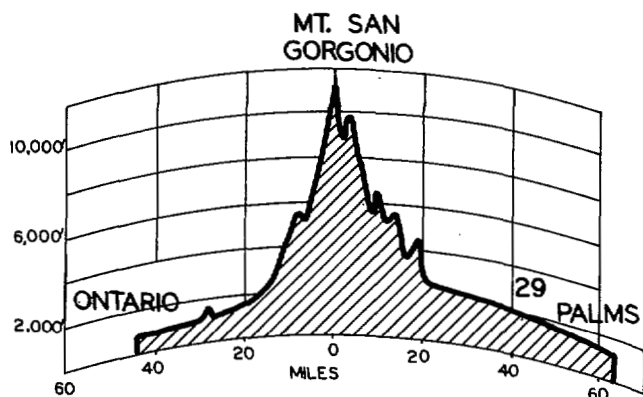


Fig. 11. Profile of single-obstacle path over Mount San Gorgonio.

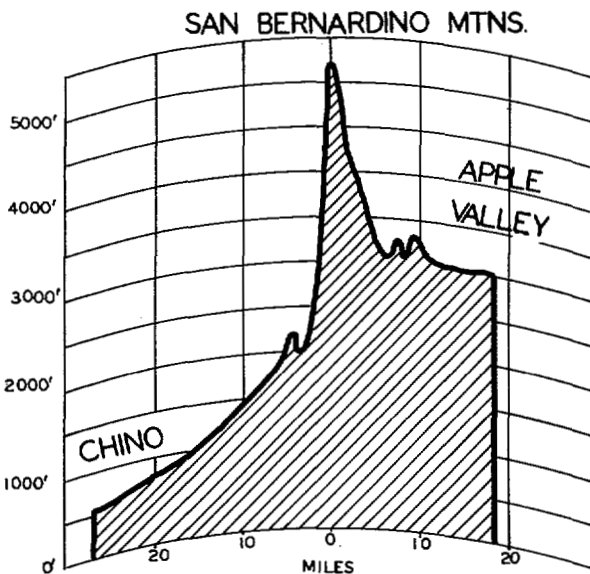


Fig. 13. Profile of single-obstacle path between Chino and Apple Valley.

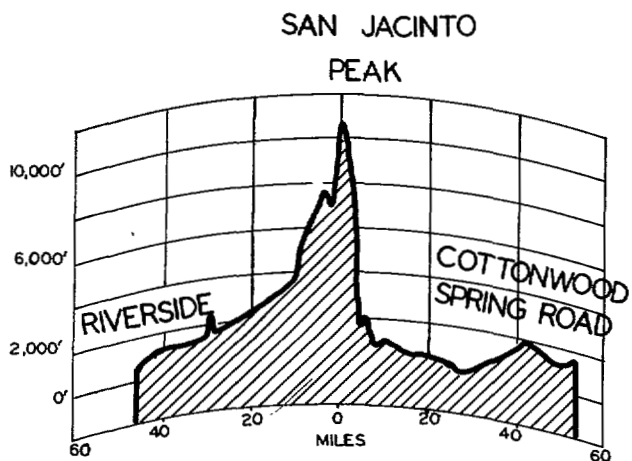


Fig. 12. Profile of single-obstacle path over Mount San Jacinto.

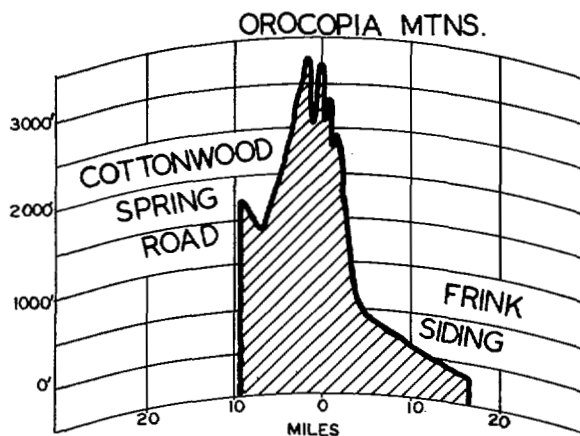


Fig. 14. Typical double-obstacle path.